

Site Response of Soft Clay Reinforced By Soil-Cement Grid Based On Dynamic Centrifuge Tests

S. Tamura¹, M. Khosravi², R. W. Boulanger³, D. W. Wilson³,
C. G. Olgun², D. Rayamajhi⁴, Y. Wang⁵

ABSTRACT

To investigate the effects of soil-cement grids reinforcement on the seismic response of soft clay sites, a series of centrifuge experiments were carried out at the UC Davis Center for Geotechnical Modeling. The following conclusions were made: (1) the average shear wave velocity of the clay with a soil-cement grid increased and it decreased less during strong shaking; (2) the soil-cement grid reduced the amplification of the clay at the natural site period but increased the amplification at the 1st higher mode period, probably because of the response of the soil-cement grid; (3) the clay without the soil-cement grid experienced large nonlinearity during strong shaking with the smaller acceleration than the clay with a soil-cement grid; (4) cracking at one side of a wall did not affect its lateral displacement, however, cracking on both sides increased its displacement amplitude but the effect on the soil displacement was negligible.

Introduction

The Deep Soil Mixing (DSM) method is a soil improvement technique that enhances soft soils by mechanically mixing them with a cementitious binder. Many construction projects use DSM to increase bearing capacity, reduce structure settlement and mitigate soil liquefaction (Almeida et al., 1985; Babasaki et al., 1991; Bradley et al., 2013; Kitazume and Terashi, 2014). The DSM method also has the potential to improve site response during earthquakes. Ishikawa and Asaka (2006) found from centrifuge tests and numerical analysis that DSM improved sand had higher natural frequencies than non-improved sand. Rayamajhi et al. (2015) investigated the natural frequencies of liquefiable sand improved by soil-cement columns. However, knowledge of the site response of clay improved by the DSM method during a large earthquake remains limited.

To investigate the effects of soil-cement grid ground reinforcement on the seismic response of soft clay sites, a series of centrifuge experiments were carried out at the UC Davis Center for Geotechnical Modeling.

¹ Dept. of Arch. and Build. Engineering, Tokyo Institute of Technology, Tokyo, Japan,
tamura@arch.titech.ac.jp

² Via Department of Civil and Environmental Engineering, Virginia Tech, Blacksburg, VA, USA,
khosravi@vt.edu, colgun@vt.edu

³ Department of Civil and Environmental Engineering, University of California, Davis, CA, USA,
rwoulanger@ucdavis.edu, dxwilson@ucdavis.edu

⁴ Department of Civil and Construction Engineering, Oregon State University, Corvallis, OR, USA,
deepak.rayamajhi@gmail.com

⁵ Key Laboratory of Earthquake Engineering and Engineering Vibration, Institute of Engineering Mechanics, CEA, Harbin, China, yong5893741@163.com

Centrifuge tests

A series of centrifuge tests was performed with a 1-m radius centrifuge at the UC Davis Center for Geotechnical Modeling using a “flexible shear beam container” under 50 g centrifugal acceleration (Khosravi et al., 2015). The inner dimensions of the container are 49.4 cm in length, 23.6 cm in width and 18 cm in depth. Figure 1 shows the test models. Model 1 is an unreinforced clay model that consists of a 12 cm (6 m in prototype scale) thick layer of coarse kaolin clay overlying a 2 cm (1m) thick bed of saturated dense sand, which is there for drainage purposes. Model 2 is the same as Model 1 but the kaolin clay is reinforced with a soil-cement grid. The soil-cement grid was placed on the dense sand layer. The kaolin clay has a liquid limit = 47, plasticity index = 19, median particle size = 4.0 μm , and a coefficient of consolidation $C_v = 0.7 \text{ mm}^2/\text{s}$ in virgin loading and $2.3 \text{ mm}^2/\text{s}$ in unloading and reloading (Stringer et al., 2012).

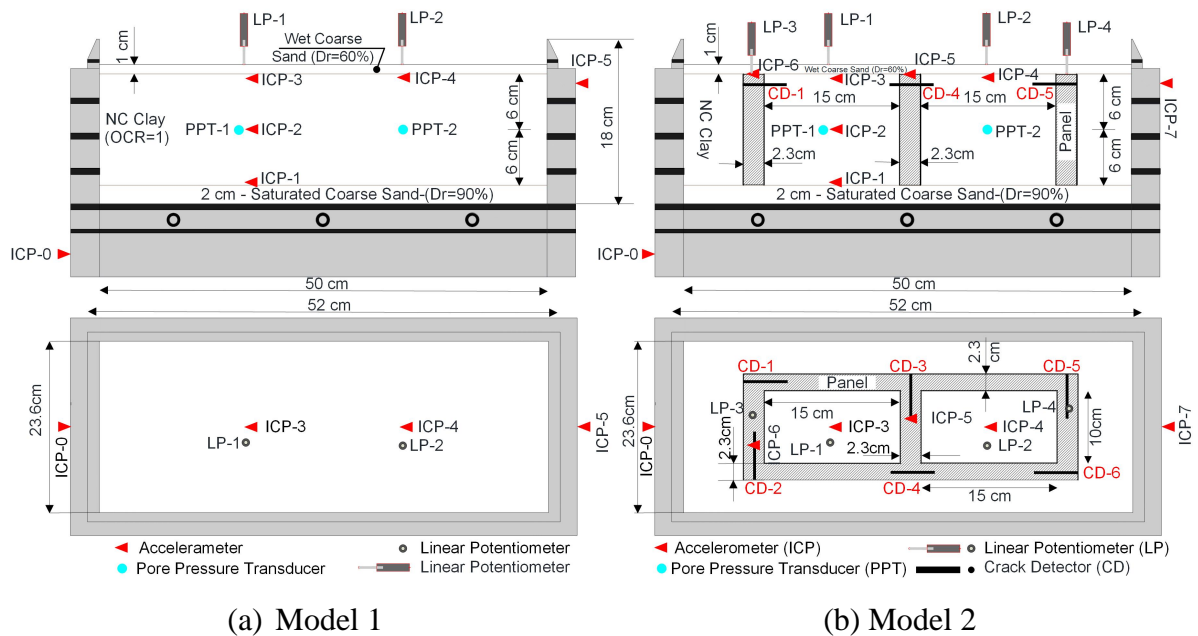


Figure 1. Test models

The clay layer in both models was made from a clay slurry with an initial water content of approximately 80% using a small vacuum mixer. The slurry was then poured into the container and pre-consolidated in a press with a vertical pressure equivalent to the self-weight of the clay at the bottom of the layer at 50 g. This process was repeated two times. The upper part of clay layers were overconsolidated by a press before performing the centrifuge tests. A thin wet sand layer was placed on the surface to prevent the clay from drying.

Clay and cement mixtures were used for the soil-cement grid construction. Several pairs of stainless steel plates were inserted into the clay model at specified spacing equal to the thickness of the soil-cement grid. The clay between the stainless steel plates was excavated and replaced with a clay-cement slurry. The weight ratio of cement, clay and water in the clay-cement slurry was 1.0, 1.9, and 3.1, respectively. After three days its unconfined compressive strength was 340-440 kPa. The width of the soil-cement wall was 2.3 cm (1.15

m) and the distance of the transverse walls (inside dimension) was 15 cm (7.5 m). The area replacement ratio was 30%.

The effect of the reinforcement on the seismic response of soft clay was investigated by comparing the response of Model 1 with Model 2. The input motions were a small sine sweep motion to check soil conditions and the 1999 Chi-Chi earthquake motion (TCU78-W) scaled to peak accelerations of 0.036g - 0.54g in prototype scale for both models. Strong sine motions were added to the shaking to investigate the effects of soil-cement damages on the site response for Model 2.

The horizontal accelerations of the soil, soil-cement grid, and box base, as well as the excess pore water pressure, settlement of the clay surface and the soil-cement grid were measured. Crack detectors were set in the soil-cement grid wall to monitor the occurrence of cracking. All test results are presented in prototype scale.

Effect of Soil-Cement Grid on Site Response

Small sine sweep motion

The effect of the soil-cement grid on the initial soil conditions was investigated by a small sine sweep motion. Peak base accelerations (PBA) were 0.007 g and 0.008 g for Models 1 and 2, respectively. The sine sweep motion contained thirty frequencies between 1 to 7Hz and 7 cycles of each frequency. Figure 2 shows spectral amplification factors for Models 1 and 2. The spectral amplification factors are the 5% damped pseudo acceleration response spectra of the ground surface motion divided by the response spectra of the motion at the top of the sand base layer. The natural periods of the clay layers for Models 1 and 2 were 0.36 s and 0.32 s, respectively. The estimated shear wave velocities based on the natural periods (T) and the relation $T=4*H/V_S$ (where H = clay layer thickness and V_S = shear wave velocity) for Models 1 and 2 were 67 m/s and 75 m/s, respectively. The average shear wave velocity of the clay layer with the soil-cement grid was 12% larger than the clay layer with no soil-cement grid.

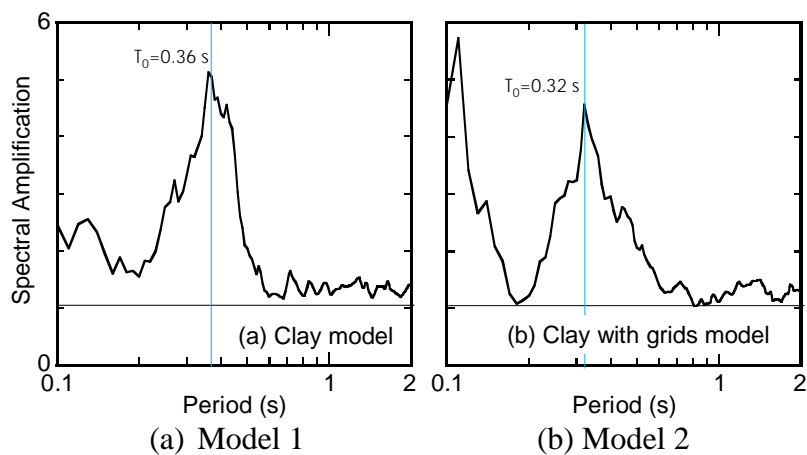


Figure 2. Spectral amplification factors for a small sine sweep motion

Small Chi-Chi motion

The Chi-Chi motion scaled to small peak accelerations was used to clarify the effect of the soil-cement grid on the clay site response during minor earthquakes. Time histories of the acceleration of the sand layer, the ground surface and the top of the soil-cement grid for Models 1 and 2 are presented in Fig. 3. PBA were 0.06 g and 0.04 g for Models 1 and 2, respectively. Peak ground accelerations (PGA) for Models 1 and 2 were 0.09 g for both models. The waveform of the clay surface acceleration in Model 2 was similar to that of the soil-cement grid, indicating that the clay response was affected by the soil-cement grid.

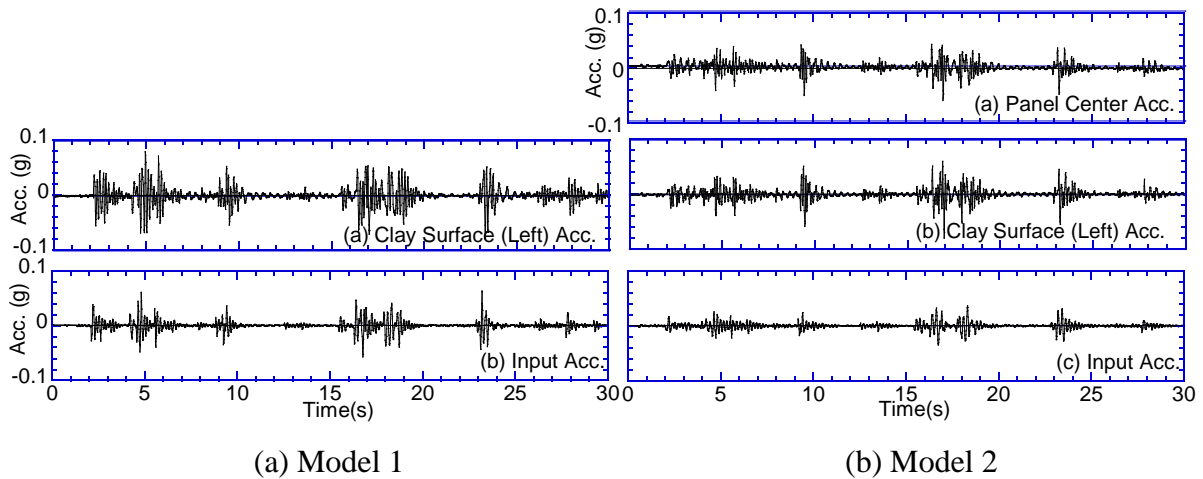


Figure 3. Time histories of the input motion and the motion at the clay surface and top of the soil-cement grid for a small Chi-Chi motion

Figure 4 shows the spectral amplification factors between the ground surface and sand base layer for Models 1 and 2. The natural periods for Models 1 and 2 are 0.48 s and 0.34 s, respectively. The estimated average shear wave velocity of the clay for Model 1 was 50 m/s, which was smaller than the initial shear wave velocity by 25%. The estimated average shear wave velocity of the clay for Model 2 was 71 m/s, which was almost the same as the initial shear wave velocity. This indicates that the soil-cement grid mitigated the nonlinearity of the clay layer. The other major peak period for Model 1 was 0.16s, corresponding to 1/3 of the natural period. Therefore, this peak is the 1st higher mode. The 1st higher mode period for Model 2 was 0.13 s. The amplification factor at the natural period for Model 2 was about half of that for Model 1. This is consistent with the fact that the impedance contrast of Model 2 is small because the soil-cement grid mitigate the reduction of the shear wave velocity of the clay layer during the shaking. On the other hand, the amplification factor at the 1st higher mode period for Model 2 was higher than that for Model 1 by 50 % in spite of the small impedance contrast. The red dotted line in the figure shows the spectral amplification factors between the top of the soil-cement grid and the sand base layer for Model 2. The amplification factor of the soil-cement grid, which is similar to the clay layer, is high near the 1st higher mode period. There is the possibility that the response of the soil-cement grid increased the clay site amplification at the 1st higher mode period.

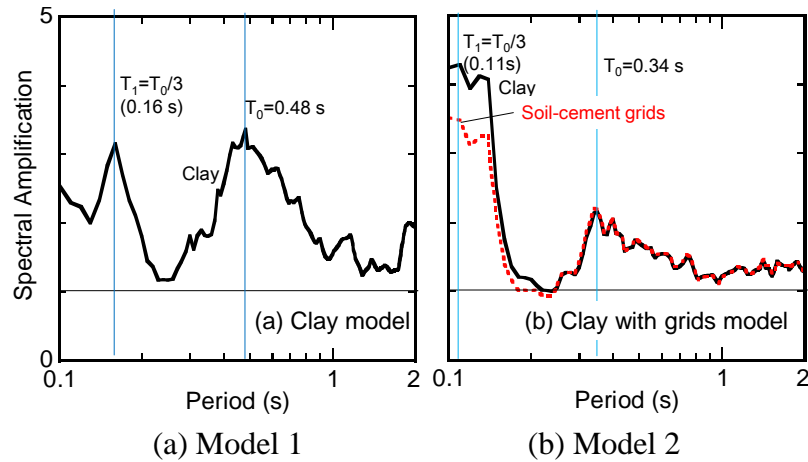


Figure 4. Spectral amplification factors for a small Chi-Chi motion

Large Chi-Chi motion

The Chi-Chi motion scaled to large peak accelerations was used to clarify the effect of the soil-cement grid on the site response during major earthquakes. Time histories of the acceleration of the sand layer, the ground surface and the top of the soil-cement grid for Models 1 and 2 are presented in Fig. 5. The PBA were 0.54 g and 0.42 g for Models 1 and 2, respectively. The acceleration amplitude of the ground surface for Model 1 was much smaller than that for Model 2. The soil-cement grid increased PGA. The waveform of the clay surface acceleration was different from that of the soil-cement grid for Model 2, indicating that the clay and soil-cement grid responses were different during strong shaking. The waveform of the soil-cement grid was similar to the sand base layer. Excess pore water pressure (EPWP) was generated during the shakings. The maximum EPWP ratios at GL-3.5 m were 0.54 and 0.56 for Models 1 and 2, respectively. The soil surface settlements were 54 mm and 56 mm for Models 1 and 2, respectively. The settlement of the soil-cement grid was only 7 mm. The EPWP and settlement of the soil with the soil-cement grid were almost the same as those of Model 1 in spite of the higher soil acceleration amplitude. The time histories of the EPWPs and the settlements are shown in the preliminary report (Khosravi et al. 2015).

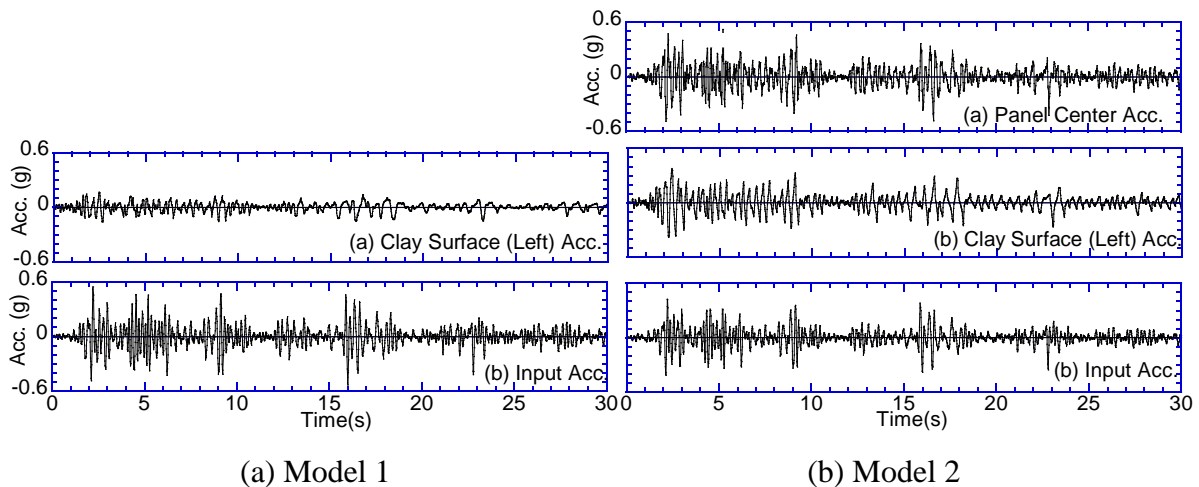


Figure 5. Time histories of the input motion and the motion at the clay surface and the top of the soil-cement grid for a large Chi-Chi motion

Figure 6 shows the spectral amplification between the ground surface and sand base layer for Models 1 and 2. The natural period for Model 1 was 1.17 s. The estimated shear wave velocity was only 21 m/s, indicating that nonlinear behavior of clay layer was extreme. The natural period for Model 2 was not clear. The amplification factor at the natural period for Model 1 was higher than that for Model 2, because of the high impedance contrast. The amplification factor at the 1st higher mode period for Model 1 was small, probably because the effect of the soil damping was dominant for the short periods.

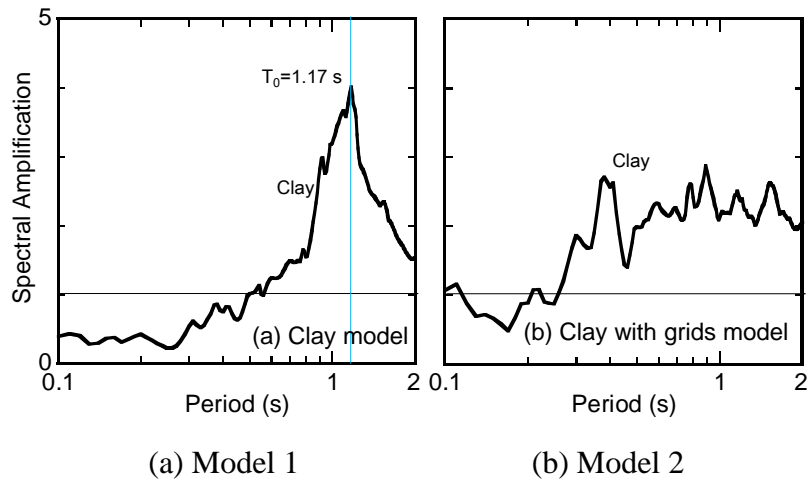


Figure 6. Spectral amplification factors for a large Chi-Chi motion

Figure 7 shows the acceleration response spectra of the clay surface and sand base layer for Models 1 and 2 to clarify the reason why the PGA for Model 1 was smaller than for Model 2 in spite of the large amplification factor at the natural period. The spectrum of the top of the soil-cement grid for Model 2 is also shown in Fig. 7(b). The predominant period of the base layer motions for both models were about 0.15-0.3 s. The amplification factor for Model 2 was about 0.6-1.8 at the predominant period as shown in Fig. 6(b). In contrast, the amplification factor for Model 1 was less than about 0.5 at the predominant period because of the high nonlinear behavior of clay layer. Therefore, the PGA for Model 1 was smaller than that for Model 2.

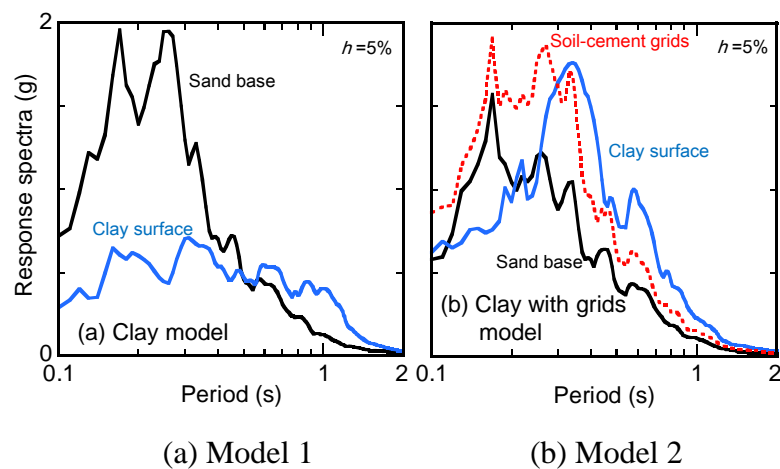


Figure 7. Pseudo acceleration response spectra for a large Chi-Chi motion

Time histories of sand layer, clay surface and soil-cement grid top for a duration of 2 seconds ($t=1-3$ s) are shown in Fig. 8. The clay surface and grid responses were almost the same until $t=2.1$ s when the base acceleration amplitudes were small. The soil-cement grid response tended to be faster than the clay response after $t=2.1$ s, indicating that seismic waves propagated the soil-cement grid. Additionally, the acceleration response spectrum of the clay surface was more like that of the soil-cement grid than that of the base layer, especially at periods shorter than 0.3 s (Fig. 7(b)). These suggest the clay surface response consisted of seismic waves propagating not only in the clay layer but also in the soil-cement grid, as shown in Fig. 9. This is consistent with the fact that the clay layer with the soil-cement grid do not have a clear natural period. The seismic wave didn't propagate well through soft clay layer because of its high damping at the short period.

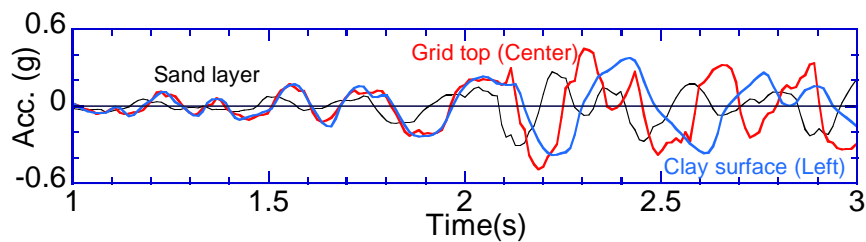


Figure 8. Time histories of sand layer, clay surface and grid

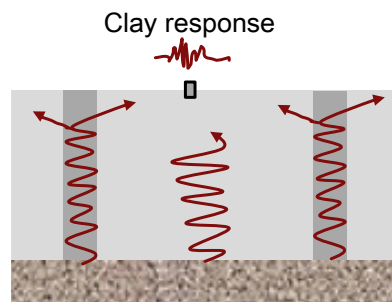


Figure. 9 Seismic waves propagating clay with the grid

Soil-Cement Grid Damage and Site Response

To investigate the damage of the soil-cement grid, a strong sine motion (frequency=2 Hz, PBA=1 g) was added for Model 2. Figure 10 shows the time histories of the clay surface and top of the soil-cement grid horizontal displacements. The displacements were estimated by double integration of acceleration. Figure 11 shows pictures of the soil-cement grid after the tests. The crack detectors indicated Crack-S and Crack-N (Fig. 11(a)) occurred at $t=9$ s and $t=14$ s, respectively. Crack-S did not affect the displacements of the clay surface and soil-cement grid. After Crack-N occurred, the displacement amplitudes of the soil-cement grid increased but that of the clay remained almost constant. The above responses indicate that cracking at one side of the wall did not affect the wall displacement. Cracking at both edges of the wall increased the displacement of the wall but had a negligible effect on the soil displacement. This test result is consistent with the numerical analysis result of Namikawa et al. (2007), which found that partial failure of improved ground is not critical in the provided level of liquefaction mitigation.

After the shaking tests, the soil surrounding the grid was excavated and the cracks in the grid were investigated. The cracks occurred at the connection points of the transverse and longitudinal walls relative to the shaking direction and in the center wall of the grid as shown in Fig. 11(a). Most cracks propagated from the top to the bottom as shown in Fig. 11(b). The cracks seem to have been caused by tensile stress due to bending.

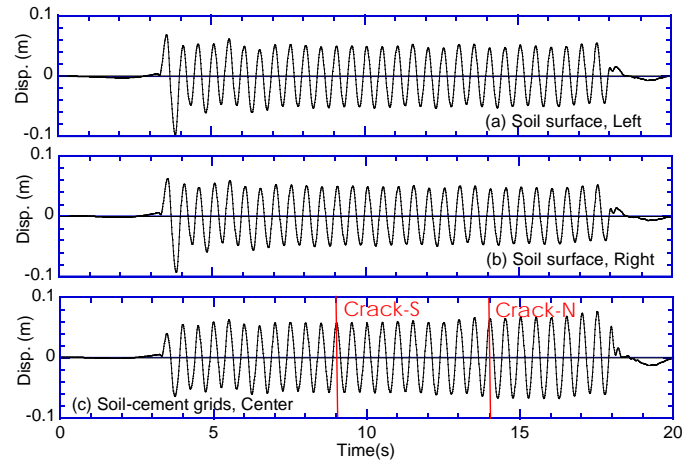


Figure 10. Time histories of displacement of clay surface and soil-cement grid top for a strong sine motion

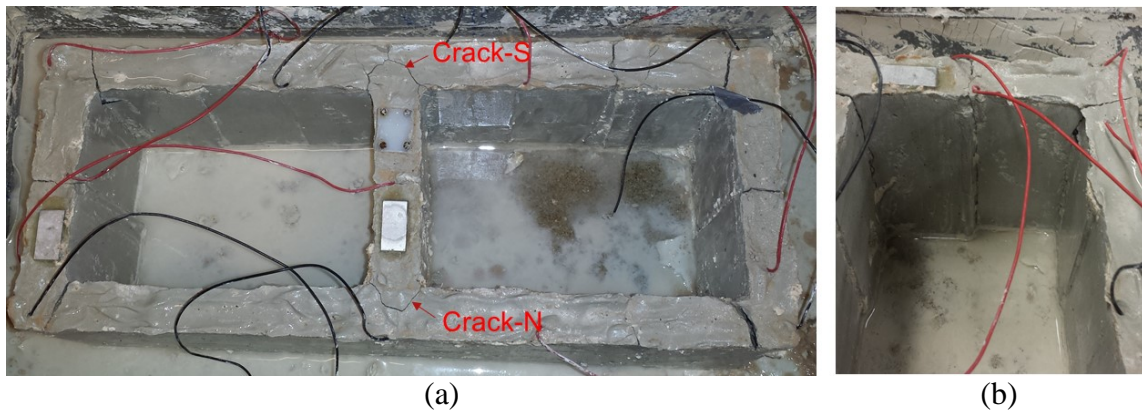


Figure 11. Pictures of the soil-cement grid after the tests

Conclusions

To investigate the effect of DSM ground reinforcement on the seismic response of soft clay sites, a series of centrifuge experiments were carried out at the UC Davis Center for Geotechnical Modeling. The following conclusions were drawn from the results of the study.

The soil-cement grid increased the average shear wave velocity of the clay layer and mitigated its nonlinearity. The soil-cement grid mitigated the seismic wave amplification of the clay at its natural site period but could not mitigate the amplification at the 1st higher mode period, probably because of the response of the soil-cement grid.

Soil nonlinearity was significant for the clay layer without the soil-cement grid during strong shaking. The natural site period changed to a period longer than the predominant period of

the input motion. Therefore, the acceleration of the clay model was smaller than that of the clay with the soil-cement grid.

Cracking in the soil-cement grid occurred during the strong sine motion. Cracking at one side of a wall did not affect its displacement. Cracking at both edges of a wall increased its displacement amplitude but had a negligible effect on the soil displacement.

Acknowledgments

This work was supported by the National Science Foundation (NSF) through the George E. Brown, Jr. Network for Earthquake Engineering Simulation (NEEScomm) under Grant No. CMMI-1208117, Pacific Earthquake Engineering Research Center (PEER), Japan Society for the Promotion of Science (JSPS) and DPRI, Kyoto University. The authors thank Dr. Brian Carlton, Tokyo Institute of Technology for insightful comments and suggestions.

References

- Almeida M. S. S., Davies M. C. R., and Parry R. H. G. "Centrifuge tests of embankments on strengthened and unstrengthened clay foundations." *Geotechnique*, 1985, **35**(4), 425-441.
- Babasaki, R., Suzuki, K., Saitoh, S., Suzuki, Y., and Tokitoh, K. "Construction and Testing of Deep Foundation Improvement Using the Deep Cement Mixing Method." *Deep Foundation Improvements: Design, Construction, and Testing*, ASTM STP 1089, 1991, Philadelphia, 224-234.
- Bradley, B.A., Araki, K., Ishii, T. and Saitoh, K. "Effect of lattice-shaped ground improvement geometry on seismic response of liquefiable soil deposits via 3-D seismic effective stress analysis." *Soil Dynamics and Earthquake Eng.*, 2013, **48**, 35-4.
- Ishikawa, A. and Asaka, Y., "Seismic responses of column and grid-type improved grounds. Physical modelling in geotechnics." *ICPMG '06 International conference; 6th, Physical modelling in geotechnics*, ICPMG '06, 2006, 521-526
- Kitazume, M. and Terashi, M. "*The Deep Mixing Method*." Taylor & Francis Group, London, UK, 410 p., 2014
- Khosravi, M., Tamura, S., Boulanger, R. W., Wilson, D. W., Olgun, C. G., Rayamajhi, D., Wang, Y. "Dynamic Centrifuge Tests on Soft Clay Reinforced by Soil-Cement Grid.", *The International Foundations Congress and Equipment Expo*, In Print., 2015.
- Namikawa, T., Koseki, J., and Suzuki, Y. "Finite element analysis of lattice-shaped ground improvement by cement-mixing for liquefaction mitigation." *Soils and Foundations*, 2007, **47**(3), 559–76.
- Rayamajhi, D., Tamura, S., Khosravi, M., Boulanger, R.W., Wilson, D., Ashford, S.A., and Olgun, C.G. "Dynamic Centrifuge Tests to Evaluate Reinforcing Mechanisms of Soil-Cement Columns in Liquefiable Sand." *J. Geotech. Geoenviron. Eng.*, 2015, 04015015.
- Stringer, M.E., Kutter, B.L., Wislon, D.W., Zhou, Y.G., and Zheng, B.L. "*Steel Pile Jacket Seismic Soil Structure Interaction Study: Phase 2 Data Report*." Center for -Geotechnical Modeling, Report No. UCD/CGMDR-12/02., 2012.